Effect of Respiration Phases on the Morphology of the Laryngopharyngeal Cavity : an Investigation Using 320-Row Area Detector ComputedTomography

ASAMI, Sae
Department of Anatomy and Physiology,Faculty of Medicine,Saga University

INAMOTO, Yoko
Faculty of Rehabilitation,School of Health Sciences, Fujita Health University

YOSHIZUKA, Hisayoshi
Department of Physical Therapy,Fukuoka International University of Health and Welfare

SAITOH, Eiichi
Department of Rehabilitation Medicine I,School of Medicine, Fujita Health University

他

https://doi.org/10.15017/4742148

出版情報：福岡醫學雜誌. 112 (3), pp.187-198, 2021-09-25. Fukuoka Medical Association
バージョン：
権利関係：

Original Article

Effect of Respiration Phases on the Morphology of the Laryngopharyngeal Cavity : an Investigation Using 320-Row Area Detector Computed Tomography

Sae Asami[1)7)], Yoko Inamoto[2)], Hisayoshi Yoshizuka[3)], Eiichi Saitoh[4)], Seiko Shibata[4)], Keiko Aihara[2)], Hitoshi Kagaya[4)], Masanao Kobayashi[5)], Toyoko Asami[6)], Akio Kuraoka[1)] and Yoshio Yamashita[7)]

[1)]*Department of Anatomy and Physiology, Faculty of Medicine, Saga University, Japan*
[2)]*Faculty of Rehabilitation, School of Health Sciences, Fujita Health University, Japan*
[3)]*Department of Physical Therapy, Fukuoka International University of Health and Welfare, Japan*
[4)]*Department of Rehabilitation Medicine I, School of Medicine, Fujita Health University, Japan*
[5)]*Faculty of Radiological Technology, School of Health Sciences, Fujita Health University, Japan*
[6)]*Department of Rehabilitation Medicine, Saga University Hospital, Japan*
[7)]*Department of Oral and Maxillofacial Surgery, Saga University, Japan*

Abstract

Purpose : The laryngopharyngeal cavity (LC) changes its shape dynamically with biological activities such as phonation, deglutition, and respiration. This study aimed to elucidate whether the laryngopharyngeal morphology changed according to the respiration phases, using data from 320-row area detector computed tomography (320-ADCT).

Materials and methods : The subjects were five healthy adult females. They underwent four single-phase respiratory synchronous volume scans with 320-ADCT during four points in the respiratory cycle : deep inspiration, deep expiration, tidal inspiration, and tidal expiration. Three-dimensional-CT images were reconstructed and used to measure the volume, length, cross-sectional area, and anteroposterior and lateral diameters of the LC. Coordinate measurements were also performed on anatomical landmarks around the LC. The data were submitted for statistical analyses.

Results : No remarkable changes were observed in the parameters during tidal respiration. The volume of the LC increased during the deep inspiration phase, with an expansion of the cross-sectional area and elongation of the anteroposterior diameter at the epiglottic vallecular level. Simultaneously, coordinate analysis revealed that the hyoid bone and tongue base moved anteriorly.

Conclusions : In this study, effect of respiration on the morphology of the LC were analyzed using 320-ADCT. The results suggested that during deep respiration, anterior deviation of the hyoid bone and tongue through the action of airway-related muscles generated dynamic movement of the pharyngeal wall, which consequently expanded the LC. It is also recommended that the tidal respiration phase is used to acquire standard values for laryngopharyngeal morphology since the LC showed stable configuration in this phase.

Key words : anatomy, computed tomography, 320-ADCT, laryngopharyngeal cavity, oropharynx, respiration

Corresponding author : Yoko Inamoto
Faculty of Rehabilitation, School of Health Sciences, Fujita Health University, 1-98 Dengakugakubo, Kutsukake, Toyoake, Aichi 470-1192, Japan
TEL : + 81-562-93-2504 FAX : + 81-562-93-4595
E-mail : inamoto@fujita-hu.ac.jp

Introduction

When performing helical CT, artifacts manifest in the direction of the anteroposterior axis because of phase changes and body movements during imaging. These artifacts reduce the precision of the obtained images. However, the 320-row area detector CT (320-ADCT), which was commercialized in 2007, enables an isochronous compatible (time is equivalent) non-helical scan with a 320-row area detector that covers a maximum range of 16 cm in a slice thickness of 0.5 mm per single tube revolution (0.275 s). This allows the acquisition of nearly static images of moving organs through high-speed scanning. It also enables the acquisition of accurate three-dimensional (3D) data of high image quality.

Moreover, dynamic volume scanning is also available by continuous tube rotations with excellent spatial-temporal resolution within a 16-cm range. Recently, this technique has been applied to 3D observation and motion analysis of the swallowing process. In eating and swallowing rehabilitation, 320-ADCT is a useful novel diagnostic and assessment tool for swallowing disorders[1)~8)].

The laryngopharyngeal cavity (LC) is essential for deglutition. A variety of studies[1)9)~14)] have reported that sex, height, and age affect the morphology of the LC. Inamoto et al., using 320-ADCT, found that the LC's volume and length were influenced by gender and height[1)]. They also hypothesized an age-related expansion of the LC because laryngoptosis associated with aging is often accompanied by elongation of the pharynx. Contrary to their hypothesis, however, the lower LC showed a tendency to decrease in volume with increasing age. Therefore, they speculated that it was because of vocal cord closure due to stopping breathing, which was found in many cases with a smaller LC[1)]. Thus, it is reasonable to consider that, in addition to gender, height, and age, the respiratory phases may also influence the morphology of the LC.

Lateral cephalometric or magnetic resonance imaging (MRI) analyses have revealed that head movement or postural change from standing to supine cause pharyngeal morphological changes[15)~17)]. Although Inoko et al. also investigated the effect of tidal respiration on the position of the hyoid bone and the anteroposterior diameter and area of the pharyngeal cavity, their cephalometric analysis revealed no remarkable changes in the oropharyngeal region[16)]. At present, however, the effect of deep respiration on laryngopharyngeal morphology has not been elucidated.

By synchronizing the 320-ADCT to respiration, it is possible to acquire nearly completely still 3D images of the laryngopharynx at any phase of respiration. This study aimed to elucidate whether the laryngopharyngeal morphology changed according to the respiration phases. By clarifying this, it may be possible to recommend the appropriate respiration phase for acquiring the standard values of laryngopharyngeal morphology, which are essential for understanding the physiology of deglutition.

Materials and methods

The subjects were five healthy adult female volunteers (mean age, 30±6 years, mean height, 159±4 cm). No subjects had any swallowing disorder or neuropathy. Following the study protocol approved by the Institutional Review Board of Fujita Health University, informed consent to participate in this study was obtained from the subjects after providing them with a complete explanation of the objective, methods, and risks of irradiation associated with this study.

Procedure

A 320-ADCT (Aquilion ONE Genesis ; Canon Medical Systems, Tochigi, Japan) was used for scanning. A seating device specially designed for CT swallowing studies, the "Offset-Sliding CT Chair" (eMedical Tokyo, Tokyo, Japan ; Tomei Brace Co., Ltd, Aichi, Japan), was placed at the

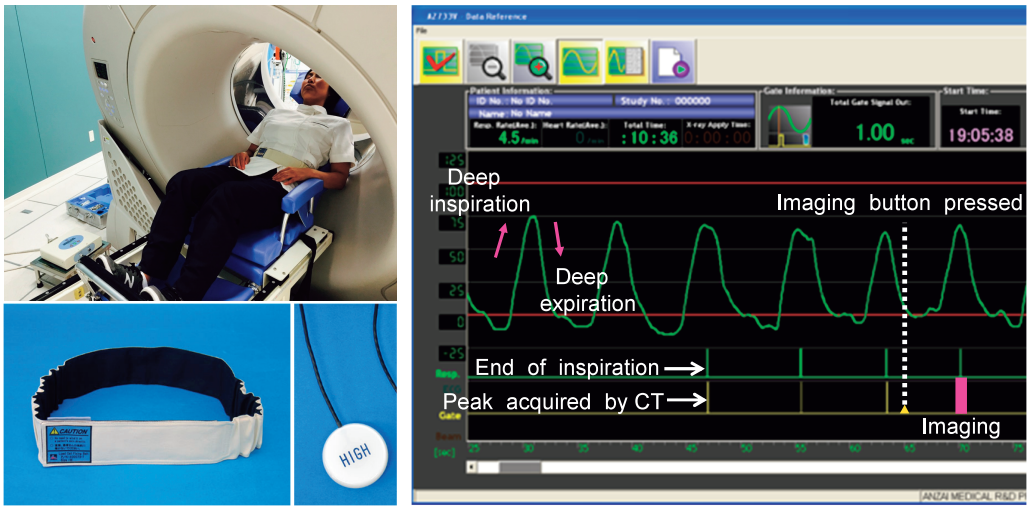

Fig. 1 Imaging method using the respiratory synchronization system
Imaging synchronized to the deep respiratory phase is shown as an example. A belt with sensors for respiration monitoring is fixed to the subject's abdomen (left panel), and the respiration waves are displayed on a screen (right panel). Once the imaging button is pressed, the next deep inspiration peak is detected and captured.

posterior opening of the CT tube. The subject was seated with the backrest at 45°. Each of the four phases of respiration (deep inspiration and expiration, and tidal inspiration and expiration) were imaged using the 320-ADCT proprietary respiration synchronization system. An abdominal belt with a pressure sensor was attached to the subject to monitor respiration. The respiratory wave was displayed on a computer screen (Fig. 1). To synchronize the timing, the subjects were instructed to perform tidal or deep respiration independently.

Once the target inspiration or expiration wave stabilized, the imaging button was pressed. Then, the next target wave was captured and used as data. Imaging was performed once for each respiratory phase to minimize radiation exposure. Imaging conditions were as follows : Imaging time was 0.275 s per phase. The imaging region was 160 mm long, extending from the base of the cranium to the upper esophagus. The slice thickness was 0.5 mm. The tube voltage/current were 120 kV/30 mA. The CT dose index and dose length product with these scanning parameters were 1.9 mGy and 30.8 mGy-cm, respectively. CT images were reconstructed using the full reconstruction method. Multiplanar reconstruction (MPR) and 3D-CT images were created using the volume-rendering method. We chose -300 HU or less to depict air column in the LC.

Measurements on morphological changes of LC

Three-dimensional measurements of the volume, length, cross-sectional area and anteroposterior and lateral diameters of the LC during each respiration phase were made using CT scanner software. To the extent possible, the measurements were based on standard anatomical nomenclature. Operational definitions for the measurements are described below (also shown in Table 1 and Fig. 2).

1. Volume and length of the LC

V-OP (Fig. 2-A) indicates the volume of upper LC. The cavity is defined as follows : bounded superiorly by the plane of the palate, which passes through the anterior nasal spine (ANS) and the posterior nasal spine (PNS) and is parallel to the infraorbital plane. The anterior boundary passes through the PNS (junction between the hard and soft palates) and is perpendicular to the plane of

Table 1 Measurement definitions

		Definition
V-OP	Volume of the upper laryngopharyngeal cavity	Bounded superiorly by the plane of the palate, which passes through the anterior nasal spine (ANS) and the posterior nasal spine (PNS), and is parallel to the infraorbital plane. The anterior boundary passes through the PNS (junction between the hard and soft palates) and is perpendicular to the plane of the palate. The inferior boundary passes through the epiglottic vallecula and is parallel to the plane of the palate.
V-LH	Volume of the lower laryngopharyngeal cavity	Predominantly surrounded by the inferior boundary of the V-OP, the upper surface of the true vocal fold, and the inferior extremity of the piriform recess.
L-OP	Upper laryngopharyngeal cavity length	The shortest distance between the superior and inferior boundaries of V-OP.
L-LH	Lower laryngopharyngeal cavity length	The shortest distance between the superior boundary of the V-LH and the superior surface of the true vocal fold.
CA-NP	Cross-sectional area at the posterior nasal spine level	The area of the cavity depicted in the axial cross-section through the PNS after imaging the ANS and PNS in the sagittal plane and adjusting so that the ANS and PNS were horizontal.
CA-SP	Cross-sectional area at the soft palate inferior extremity level	The area of the cavity depicted in the axial cross-section, which passes through the inferior extremity of the soft palate in the mid-sagittal section, and is parallel to the cross-sectional image for CA-NP.
CA-VAL	Cross-sectional area at the vallecular level	The area of the cavity depicted in the axial cross-section, which passes through the bottom of vallecula in the mid-sagittal section, and is parallel to the cross-sectional image for CA-NP.
CA-TVC	Cross-sectional area at the true vocal cord level	The area of the cavity depicted in the axial cross-section through the bilateral vocal processes of the arytenoid cartilages after adjusting the vocal cords to horizontal in the sagittal section.
AP-SP	Anteroposterior diameter at the soft palate inferior extremity level	The distance between the anterior cavity wall commissure and the boundary at the most dorsal point in the same cross-sectional image for CA-SP.
AP-VAL	Anteroposterior diameter at the vallecular level	The distance between the anterior cavity wall commissure and the boundary at the most dorsal point in the same cross-sectional image for CA-VAL.
AP-TVC	Anteroposterior diameter at the true vocal cord level	The distance between the anterior cavity wall commissure and the boundary at the most dorsal point in the same cross-sectional image for CA-TVC.
L-SP	Lateral diameter at the soft palate inferior extremity level	The maximum lateral width of the cavity in the same cross-sectional image for CA-SP.
L-VAL	Lateral diameter at the vallecular level	The maximum lateral width of the cavity in the same cross-sectional image for CA-VAL.

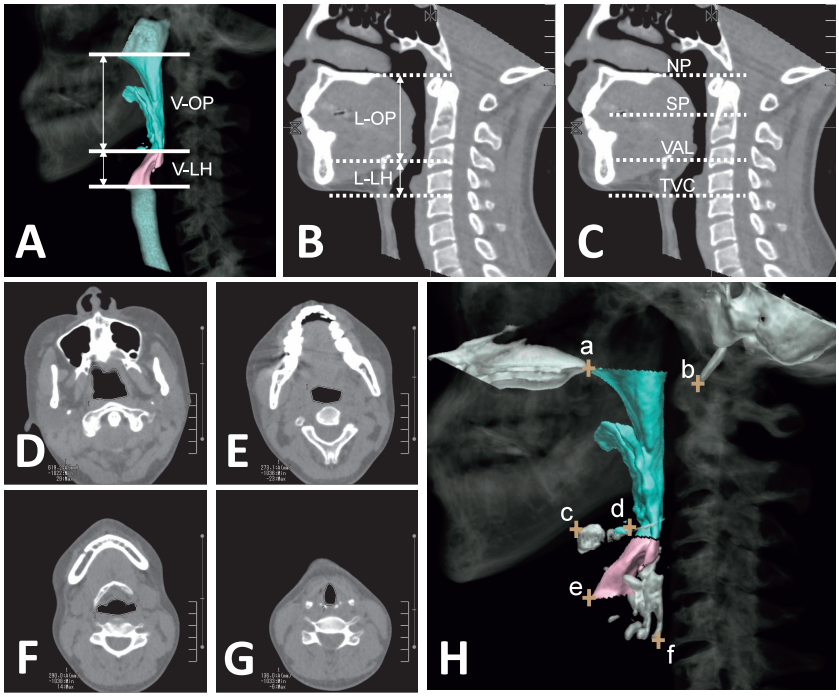

Fig. 2 Defining structural measurements using multiplanar reconstruction (MPR) and 3D-CT images
A) An MPR image of the laryngopharyngeal cavity (LC). V-OP, volume of the upper LC ; V-LH, volume of the lower LC. **B**, **C**) Sagittal-sectional 3D-CT images of LC. L-OP, the upper LC length ; L-LH, the lower LC length ; NP, the posterior nasal spine (PNS) level ; SP, the soft palate inferior extremity level ; VAL, the epiglottic vallecular level ; TVC, the true vocal cord level. **D**-**G**) Cross-sectional 3D-CT images of LC. Each figure corresponds to the levels indicated in **C** : **D**), NP ; **E**), SP ; **F**), VAL ; **G**), TVC. **H**) An MPR image of LC. Locations of the PNS (a), styloid (b), hyoid bone (c), tongue base (d), true vocal cords (e), and inferior extremity of thyroid cartilage (f) are indicated.

the palate. The inferior boundary passes through the epiglottic vallecula and is parallel to the plane of the palate.

V-LH (Fig. 2-A) indicates the volume of the lower LC. It is impossible to confidently mark the soft tissue border between the hypopharynx and the supraglottic larynx. Thus, the cavity was defined as an area predominantly surrounded by the inferior boundary of the V-OP, the upper surface of the true vocal fold, and the inferior extremity of the piriform recess.

The lengths of the upper and lower LC were denominated as L-OP and L-LH, respectively (Fig. 2-B). L-OP is the shortest distance between the superior and inferior boundaries of V-OP. L-LH is the shortest distance between the superior boundary of the V-LH and the superior surface of the true vocal fold.

2. Cross-sectional area and diameters of LC

To define the cross-sectional area at the PNS level (CA-NP), at the soft palate inferior extremity level (CA-SP), and the epiglottic vallecular level (CA-VAL), the ANS and PNS were imaged in the sagittal plane and adjusted so that the ANS and PNS were horizontal. Axial cross-sections were then performed in accordance with the PNS (Fig. 2-C, D), inferior extremity of the soft palate in the mid-sagittal section (Fig. 2-C, E), and the bottom of the vallecula in the mid-sagittal section (Fig. 2-C, F). To define the cross-sectional area at the true vocal cord level (CA-TVC), the vocal cords were adjusted to horizontal in the sagittal section, and an axial cross-section was made in

which the bilateral vocal processes of the arytenoid cartilages were imaged (Fig. 2-C, G).

The anteroposterior diameter of the LC was defined as the distance between the anterior cavity wall commissure and the boundary at the most dorsal point. In this study, measurements were performed on three cross-sections : at the soft palate inferior extremity level (AP-SP), at the vallecular level (AP-VAL), and the true vocal cord level (AP-TVC).

The lateral diameter was defined as the maximum lateral width. The cross-sections were measured at the soft palate inferior extremity level (L-SP) and the vallecular level (L-VAL).

Coordinate measurement

Coordinate measurements were performed to investigate the movement of anatomical landmarks around the LC during respiration. The Y-axis was defined as the line passing through the anterior-inferior corner of the C2 and anterior-superior corner of the C4 vertebral bodies, on the mid-sagittal section. The intersection of the coordinate axes, anterior-superior corner of the C4 vertebral body, was set as (x, y) = (0, 0). As shown in Fig. 2-H, posterior-superior corner of the PNS, inferior extremity of the styloid process, anterior-superior corner of the hyoid bone body, most posterior portion of the tongue base facing the epiglottis vallecula, anterior extremity of the vocal cord, and inferior extremity of the thyroid cartilage were tracked using the x and y coordinates.

Statistical analysis

All statistical analyses were performed using IBM SPSS Statistics version 22. A p-value of less than 0.05 was considered statistically significant. Average values of volume, length, cross-sectional area, anteroposterior and lateral diameters of the LC, and coordinate data during each respiratory phase were calculated and compared. The Shapiro-Wilk and Levene tests were used to check their normality and homogeneity, respectively. Normal and homogeneous data were analyzed by one-way analysis of variance (ANOVA) and post hoc Tukey's test, and non-normally distributed data were analyzed with the Kruskal-Wallis test.

Results

Table 2 shows the data on the volume and length of the LC. No remarkable changes were observed between the respiration statuses for V-LH, L-OP, and L-LH. The change of V-OP was also unremarkable during tidal respiration but increased during deep respiration in all subjects. The maximum values were always observed at the deep inspiration phase. A particularly large change was observed in subject 1, where the V-OP reached 2.2 times the tidal expiration value. However, the deep inspiration to deep expiration V-OP change ratio varied from 110.9% to 169.2% among the subjects. To pursue this issue further, we compared the cross-sectional areas of each subject (Fig. 3). Subjects 3 and 5 showed an increase of CA-SP and CA-VAL only in deep inspiration, while subjects 1 and 4 showed a similar pattern of increases in deep inspiration and expiration. No value for CA-NP was detected in subject 1 at deep expiration. This was probably due to the complete closure of LC by the soft palate.

The average data of each parameter are shown in Table 3. A trend toward increasing in deep inspiration was noticed in V-OP, CA-SP, AP-SP, L-SP and L-VAL. However, a significant increase was detected only in CA-VAL ($p < 0.05$, vs tidal inspiration and expiration) and AP-VAL ($p < 0.05$, vs deep expiration ; $p < 0.01$, vs tidal inspiration ; $p < 0.001$, vs tidal expiration).

Table 4 shows the average changes in positional relation to the anatomical landmarks during each respiration phase. Though no significant change was detected, all the structures tended to be deviated superiorly during deep respiration, probably due to an unpredictable head motion during imaging. It was noteworthy that the hyoid bone and tongue base deviated anteriorly during

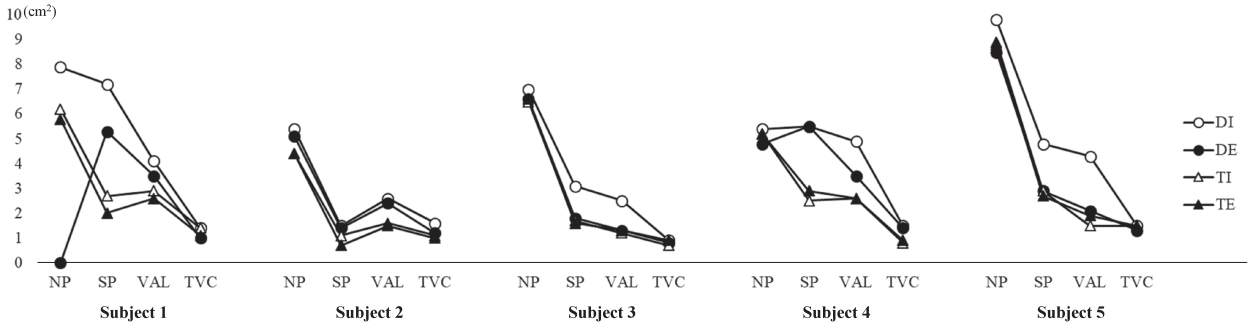

Fig. 3 Individual variability of cross-sectional area at the different respiratory phases
The cross-sectional area of each subject is plotted at different pharyngeal levels for deep inspiration (DI), deep expiration (DE), tidal inspiration (TI), and tidal expiration (TE). Note that subjects 3 and 5 showed a similar pattern, while the patterns of other subjects were somewhat different, especially at the soft palate inferior extremity level (SP) and the vallecular level (VAL). NP, posterior nasal spine level ; TVC, true vocal cord level.

Table 2 Measured volume and length of the laryngopharyngeal cavity in each subject

Subjects			1	2	3	4	5
	Sex		F	F	F	F	F
	Age	yr	35	37	33	23	22
	BMI	kg/m^2	19.8	27.0	19.3	20.4	20.8
V-OP	Deep inspiration	cm^3	28.7	9.3	16.1	20.4	22.5
	Deep expiration	cm^3	17.6	6.6	11.6	18.4	13.3
	Ratio (inspiration/expiration)	%	163.1	140.9	138.8	110.9	169.2
	Tidal inspiration	cm^3	14.1	5.9	11.8	11.9	16.3
	Tidal expiration	cm^3	13.1	5.6	11.3	12.6	16.4
	Ratio (inspiration/expiration)	%	107.6	105.4	104.4	94.4	99.4
V-LH	Deep inspiration	cm^3	6.0	3.8	3.4	6.8	7.5
	Deep expiration	cm^3	5.6	2.8	2.7	5.6	5.1
	Ratio (inspiration/expiration)	%	107.1	135.7	125.9	121.4	147.1
	Tidal inspiration	cm^3	4.7	3.6	3.3	4.6	4.7
	Tidal expiration	cm^3	4.4	3.1	3.0	4.6	5.2
	Ratio (inspiration/expiration)	%	106.8	116.1	110.0	100.0	90.4
L-OP + L-LH	Deep inspiration	mm	72.1	74.8	76.1	72.2	67.6
	Deep expiration	mm	71.6	70.5	73.6	73.6	62.0
	Ratio (inspiration/expiration)	%	100.7	106.1	103.4	98.1	109.0
	Tidal inspiration	mm	73.0	72.0	75.1	76.3	67.6
	Tidal expiration	mm	73.0	74.8	70.8	76.4	66.9
	Ratio (inspiration/expiration)	%	100.0	96.3	106.1	99.9	101.0

V-OP : Volume of the upper laryngopharyngeal cavity ; V-LH : Volume of the lower laryngopharyngeal cavity ;
L-OP : Upper laryngopharyngeal cavity length ; L-LH : Lower laryngopharyngeal cavity length.

Table 3 Average dimensions of parameters at each respiratory phase (n = 5)

		Mean ± SD				ANOVA	
		Deep Inspiration	Deep Expiration	Tidal Inspiration	Tidal Expiration	*f*	*p*
V-OP	cm^3	19.4 ± 7.2	13.5 ± 4.8	12.0 ± 3.9	11.8 ± 3.9	2.40	0.11
V-LH	cm^3	5.5 ± 1.8	4.4 ± 1.5	4.2 ± 0.7	4.1 ± 1.0	-	0.42
L-OP	mm	50.6 ± 3.0	48.8 ± 4.1	49.5 ± 2.3	50.3 ± 2.7	0.36	0.78
L-LH	mm	21.9 ± 1.9	21.5 ± 2.6	23.3 ± 2.7	22.1 ± 2.8	0.49	0.69
CA-NP	cm^2	7.1 ± 1.9	5.0 ± 3.2	6.2 ± 1.7	6.2 ± 1.7	0.79	0.52
CA-SP	cm^2	4.4 ± 2.2	3.4 ± 1.9	2.2 ± 0.8	2.0 ± 0.9	2.54	0.09
CA-VAL	cm^2	3.7 ± 1.1	2.6 ± 1.0	2.0 ± 0.8[a]	2.0 ± 0.6[b]	4.29	< 0.05
CA-TVC	cm^2	1.4 ± 0.3	1.1 ± 0.3	1.1 ± 0.3	1.1 ± 0.2	-	0.22
AP-SP	mm	12.7 ± 5.8	12.6 ± 7.7	8.8 ± 2.4	8.2 ± 2.4	1.13	0.37
AP-VAL	mm	15.1 ± 1.9	11.1 ± 2.5[c]	9.0 ± 2.0[d]	8.6 ± 1.9[e]	10.05	< 0.001
AP-TVC	mm	16.3 ± 0.8	15.1 ± 0.5	15.6 ± 0.7	15.7 ± 0.6	-	0.07
L-SP	mm	28.3 ± 9.0	24.6 ± 5.5	22.6 ± 5.2	22.8 ± 6.3	0.80	0.51
L-VAL	mm	34.1 ± 2.6	29.4 ± 5.3	26.8 ± 6.2	26.8 ± 7.1	1.91	0.17

[a] Deep Inspiration vs. Tidal Inspiration : $p < 0.05$. [b] Deep Inspiration vs. Tidal Expiration : $p < 0.05$.
[c] Deep Inspiration vs. Deep Expiration : $p < 0.05$. [d] Deep Inspiration vs. Tidal Inspiration : $p < 0.01$.
[e] Deep Inspiration vs. Tidal Expiration : $p < 0.001$.

Table 4 Average coordinate position of anatomical landmarks at each respiratory phase (n = 5)

		Mean ± SD (mm)				ANOVA	
		Deep Inspiration	Deep Expiration	Tidal Inspiration	Tidal Expiration	*f*	*p*
PNS	X	−32.2 ± 4.7	−31.9 ± 3.5	−32.3 ± 4.6	−33.2 ± 4.9	0.08	0.97
	Y	73.0 ± 6.2	69.5 ± 5.7	65.8 ± 5.7	65.9 ± 5.0	-	0.25
Styloid	X	3.1 ± 8.2	4.2 ± 8.8	4.7 ± 7.5	3.4 ± 8.8	0.04	0.99
	Y	63.0 ± 7.4	61.1 ± 5.9	59.5 ± 4.5	60.1 ± 5.1	0.34	0.80
Hyoid bone	X	−34.1 ± 1.4	−32.1 ± 1.7	−31.0 ± 2.5	−30.5 ± 2.3	3.13	0.05
	Y	23.1 ± 9.1	21.7 ± 6.9	18.1 ± 5.5	17.8 ± 5.6	0.72	0.55
Tongue base	X	−21.2 ± 3.2	−17.9 ± 4.6	−16.9 ± 2.8	−15.9 ± 1.8	2.52	0.09
	Y	23.8 ± 7.8	24.3 ± 7.3	19.2 ± 4.5	19.5 ± 4.6	0.95	0.44
Vocal cords	X	−24.6 ± 1.2	−24.2 ± 0.8	−24.0 ± 1.9	−24.1 ± 2.2	0.13	0.94
	Y	−1.9 ± 6.5	−0.7 ± 5.4	−7.0 ± 3.8	−6.7 ± 4.4	2.03	0.15
Thyroid cartilage inferior extremity	X	−9.6 ± 2.5	−9.2 ± 1.9	−8.2 ± 3.2	−8.4 ± 3.0	0.30	0.83
	Y	−10.6 ± 6.2	−11.2 ± 4.0	−16.2 ± 3.6	−16.1 ± 4.7	2.06	0.15

The anterior-superior corner of the C4 vertebral body was set as (x, y) = (0, 0). Minus (−) values on the X-axis indicate anterior and plus (+) values indicate posterior directionality. Plus (+) values on the Y-axis indicate superior and minus (−) values indicate inferior directionality.

deep respiration. Compared to tidal expiration, their forward deviations were 3.6 mm and 5.3 mm for the hyoid bone and tongue base, respectively.

Discussion

Inamoto et al. found, using 320-ADCT, that the volume and length of LC were related to height and sex, with men having a larger laryngopharyngeal volume than women. Regarding age, the volume of the lower LC significantly decreased with age[1]. On the other hand, MRI analysis by Malhotra et al. showed that the LC is elongated in older individuals. The difference in men and women was 4.2 mm and 8.0 mm, respectively[12]. Shigeta et al. showed that the entire length of the oropharynx increased by 0.428 mm/year in men and 0.153 mm/year in women[13]. Conversely, Schendel et al. revealed that both the volume and length of the oropharynx gradually decreased after the age of 20 and then rapidly decreased after the age of 40[14]. Those previous reports suggest the possible effect of gender and aging on LC. Therefore, the subjects in this study were limited to young females.

The increase of V-OP during deep inspiration, observed in all subjects, was considered reasonable for reducing the resistance during inspiration. Given that CA-VAL and AP-VAL were significantly increased and the hyoid bone and tongue base displaced more anteriorly during deep inspiration, it is suggested that the increase in laryngopharyngeal volume was caused mainly by the anteroposterior expansion of the airway at the level of the epiglottic vallecula. Previous studies have reported that airway-associated muscles such as the lingual muscle and the suprahyoid and infrahyoid muscle groups help maintain the airway during respiration. In particular, during the inspiration phase, it is known that the tongue and hyoid bone are pulled anteriorly[18)~20)], as confirmed in this study. Changes in muscular activity in the tongue's extrinsic muscles (hyoglossus, genioglossus, and styloglossus) or suprahyoid muscles (digastric, geniohyoid, mylohyoid, and stylohyoid) may have influenced the anterior movement of the tongue and hyoid bone, causing expansion of the LC. This concept should be addressed further in future studies.

We also confirmed the individual variability in cross-sectional areas across four respiratory phases. Namely, the behavior of CA-SP and CA-VAL at the deep expiration phase was different between subjects. This result might have affected the variance of the ratio of V-OP change at deep inspiration to the change at deep expiration. The result also suggested there might be individual differences in the muscle activity underlying airway patency variability. In addition, the cross-sectional area of subject 2 did not show prominent changes across the respiration phases. This could be explained by the effect of subject 2's body mass index (27.0), categorized as obese. Fewer individual variations were found during tidal respiration than during deep respiration. The tidal phase is therefore recommended for acquiring standard values for laryngopharyngeal morphology.

This study had several limitations. One was that anatomical landmarks such as the PNS were elevated during deep inspiration, possibly resulting from unpredictable head motion. Future studies will need to compensate for this. Next, the scanning conditions, such as the number of scans, need to be considered carefully to avoid the risk of radiation exposure. In addition, our sample was limited to young females to eliminate the effect of gender differences in the LC and vocal cords. Though all subjects increased LC volume during deep breathing, there may be some females whose respiratory waveforms are poorly detected by the abdomen sensor due to their thoracic respiration pattern. In the future, therefore, we need studies to include male and elderly subjects to deepen our understanding on the relationship between pharyngeal structure and respiration.

The potential use of the 320-ADCT for analysis of the LC during respiration includes research

into the sleep apnea syndrome[21)22)]. Acoustic pharyngometry, which is commonly used in the diagnosis and study of sleep apnea syndrome, has recently been assessed in the field of swallowing research[23)]. Thus, 320-ADCT may prove useful in confirming the validity of acoustic pharyngometry measurements.

Acknowledgments

We greatly appreciate the members of the Department of Rehabilitation Medicine I and the Faculty of Rehabilitation at Fujita Health University, as well as the Radiology Department of Fujita Health University Hospital for their continuous support during this research. We also express our sincere gratitude to Editage (www.editage.jp) for English language editing.

Conflict of interest

The authors declare that they have no conflict of interest.

References

1) Inamoto Y, Saitoh E, Okada S, Kagaya H, Shibata S, Baba M, Onogi K, Hashimoto S, Katada K, Wattanapan P and Palmer JB : Anatomy of the larynx and pharynx : effects of age, gender and height revealed by multidetector computed tomography. J. Oral Rehabil. 42 : 670-677, 2015.
2) Inamoto Y, Saitoh E, Ito Y, Kagaya H, Aoyagi Y, Shibata S, Ota K, Fujii N and Palmer JB : The Mendelsohn maneuver and its effects on swallowing : kinematic analysis in three dimensions using dynamic area detector CT. Dysphagia 33 : 419-430, 2018.
3) Kanamori D, Kagaya H, Fujii N, Inamoto Y, Nakayama E, Suzuki S, Mizutani H, Okada S, Katada K and Saitoh E : Examination of the distance measurement error and exposed dose when using a 320-row area detector CT : a comparison with videofluoroscopic examination of swallowing. Jpn. J. Compr. Rehabil. Sci. 2 : 18-23, 2011.
4) Inamoto Y, Saitoh E, Okada S, Kagaya H, Shibata S, Ota K, Baba M, Fujii N, Katada K, Wattanapan P and Palmer JB : The effect of bolus viscosity on laryngeal closure in swallowing : kinematic analysis using 320-row area detector CT. Dysphagia 28 : 33-42, 2013.
5) Fujii N, Inamoto Y, Saitoh E, Baba M, Okada S. Yoshioka S, Nakai T, Ida Y, Katada K and Palmer JB : Evaluation of swallowing using 320-detector-row multislice CT. Part Ⅰ : single-and multiphase volume scanning for three-dimensional morphological and kinematic analysis. Dysphagia 26 : 99-107, 2011.
6) Inamoto Y, Fujii N, Saitoh E, Baba M, Okada S, Katada K, Ozeki Y, Kanamori D and Palmer JB : Evaluation of swallowing using 320- detector-row multislice CT. Part Ⅱ : kinematic analysis of laryngeal closure during normal swallowing. Dysphagia 26 : 209-217, 2011.
7) Okada T, Aoyagi Y, Inamoto Y, Saitoh E, Kagaya H, Shibata S. Ota K and Ueda K : Dynamic change in hyoid muscle length associated with trajectory of hyoid bone during swallowing : analysis using 320-row area detector computed tomography. J. Appl. Physiol. 115 : 1138-1145, 2013.
8) Nakayama E, Kagaya H, Saitoh E, Inamoto Y, Hashimoto S, Fujii N, Katada K, Kanamori D, Tohara H and Ueda K : Changes in pyriform sinus morphology in the head rotated position as assessed by 320-row area detector CT. Dysphagia 28 : 199-204, 2013.
9) Sato K : Three dimensional anatomy of the larynx : investigation by whole organ sections. Jibi. 33 : 153-182 (in Japanese with English summary), 1987.
10) Kiyokawa K : Effects of intrinsic laryngeal muscles to the glottis : experimental study of the excised human larynges. Jibi. 33 : 187-217 (in Japanese with English summary), 1987.
11) Ara A, Khalil M, Sultana SZ, Ahmed MS, Akhter F, Haque N, Haque MA and Choudhury AI : Morphometric study of vocal fold of different sexes of Bangladeshi cadaver. Mymensingh Med. J. 19 : 173-175, 2010.
12) Malhotra A, Huang Y, Fogel R, Lazic S, Pillar G, Jakab M, Kikinis R and White DP : Aging influences on pharyngeal anatomy and physiology : the predisposition to pharyngeal collapse. Am. J. Med. 119 : 72.e9-72.e14, 2006.
13) Shigeta Y, Ogawa T, Venturin J, Nguyen M, Clark GT and Enciso R : Gender- and age-based differences in computerized tomographic measurements of the oropharynx. Oral Surg. Oral Med. Oral Pathol. Oral Radiol. Endod. 106 : 563-570, 2008.
14) Schendel SA, Jacobson R and Khalessi S :

Airway growth and development : a computerized 3-dimensional analysis. J. Oral Maxillofac. Surg. 70 : 2174-2183, 2012.
15) Nagai M, Kudo A, Matsuno I, Yokoyama M, Manabe J, Hasegawa S and Nakamura S : Hyoid bone position and airway accompanied with influence of head posture. J. Jpn. Orthod. Soc. 48 : 214-225 (in Japanese with English summary), 1989.
16) Inoko Y, Takahashi F, Ohnuma T and Morita O : Influence of posture and respiration on the morphology of oropharynx : analysis by cephalometric radiogram. J. Jpn. Prosthodont. Soc. 47 : 508-515 (in Japanese with English summary), 2003.
17) Inoko Y, Takahashi F, Ohnuma T, Morita O, Sasaki Y and Tsuchimochi M : Influence of anteflexion of head position on the shape of pharyngeal space by magnetic resonance imaging. J. Jpn. Prosthodont. Soc. 46 : 28-33 (in Japanese with English summary), 2002.
18) Brouillette RT and Thach BT : Control of genioglossus muscle inspiratory activity. J. Appl. Physiol. 49 : 801-808, 1980.
19) Brouillette RT and Thach BT : A neuromuscular mechanism maintaining extrathoracic airway patency. J. Appl. Physiol. 46 : 772-779, 1979.
20) Cheng S, Butler JE, Gandevia SC and Bilston LE : Movement of the tongue during normal breathing in awake healthy humans. J. Physiol. 586 : 4283-4294, 2008.
21) Ying B, Huang Q, Su Y, Fu B. Ye X, Huang Y and Li Z : 320-detector CT imaging of the upper airway structure of patients with obstructive sleep apnea-hypopnea syndrome. J. Craniofac. Surg. 23 : 675-677, 2012.
22) Guilleminault C, Hill MW, Simmons FB and Dement WC : Obstructive sleep apnea : electromyographic and fiberoptic studies. Exp. Neurol. 62 : 48-67, 1978.
23) Molfenter SM : The reliability of oral and pharyngeal dimensions captured with acoustic pharyngometry. Dysphagia 31 : 555-559, 2016.

(Received for publication December 18, 2020)

（和文抄録）

咽頭喉頭腔の形態に対する呼吸時相の影響について：320 列面検出器型 CT を用いた検討

[1)]佐賀大学医学部　解剖学・人類学分野
[2)]藤田医科大学保健衛生学部　リハビリテーション学科
[3)]福岡国際医療福祉大学医療学部　理学療法学科
[4)]藤田医科大学医学部　リハビリテーション医学Ⅰ講座
[5)]藤田医科大学医療科学部　放射線学科
[6)]佐賀大学医学部附属病院　リハビリテーション科
[7)]佐賀大学医学部　歯科口腔外科学講座

浅見紗衣[1)7)]，稲本陽子[2)]，吉塚久記[3)]，才藤栄一[4)]，柴田斉子[4)]，
粟飯原けい子[2)]，加賀谷　斉[4)]，小林正尚[5)]，浅見豊子[6)]，
倉岡晃夫[1)]，山下佳雄[7)]

目的：咽頭喉頭腔（LC）は，発声，嚥下，呼吸などの活動状況によってその形態が変化する．本研究では，320 列面検出器型 CT（320-ADCT）を用いて，様々な呼吸時相が LC の形態に変化を及ぼすか否かを明らかにすることを目的とした．

材料と方法：5 名の健常成人女性を被験者とし，呼吸サイクルの 4 時相（深吸気，深呼気，安静吸気，安静呼気）を，320-ADCT 付属の呼吸同期システムを用いて，各 1 回ずつ 1 時相にて撮像した．3D-CT 画像を作成した後，LC の体積，長さ，断面積，および前後・左右径を計測した．また，LC 周辺の解剖学的指標について座標の変化を計測し，統計解析を行った．

結果：安静呼吸時において計測値の変動は特に認めなかったが，深吸気時において LC の体積は増加し，喉頭蓋谷レベルの断面像における内腔面積の増加と前後径の伸長が認められた．座標分析では，深吸気時における舌骨と舌根部の前方への移動が認められた．

結論：320-ADCT を用いて LC の形態に対する呼吸の影響を検討した結果，深吸気時において LC の拡大が認められ，おそらくは気道関連筋群の作用による舌骨と舌の前方への移動が咽頭壁の動的な変化をもたらし，この現象が生じたことが示唆された．また，安静呼吸時に LC の形態が比較的安定していたことから，咽頭喉頭腔に関する標準的な計測値を得る呼吸時相として適切と考えられる．

キーワード：生体構造，コンピュータ断層撮影，320 列面検出器型 CT，咽頭喉頭腔，咽頭口部，呼吸